3CSCE Annual Conference
Growing with youth – Croître avec les jeunes

Laval (Greater Montreal)
June 12 - 15, 2019

Experimental investigation on the bending behaviour of exterior beam-column connections made with Engineered Cementitious Composite

A. Ehsani Yeganeh[1,2], K. M. A. Hossain[1,3],
[1] Department of Civil Engineering, Ryerson University, Canada
[2] Ali.ehsaniyeganeh@ryerson.ca, [2] ahossain@ryerson.ca

Abstract: Structural performance of exterior reinforced beam-column connections made with Engineered Cementitious Composite (ECC) under bending is investigated experimentally and compared with those made of Self-Consolidating Concrete (SCC). Beam-column connections of 1/3rd scale made entirely of ECC, SCC and ECC-SCC combination (beam-column connection core zone made of ECC while rest of the specimen made with SCC) were tested under monotonic bending loading to failure. The performance is compared in terms of failure mode, ductility, energy absorption capacity, stiffness, moment-rotation response, stress-strain characteristics, crack patterns, number of cracks and crack widths. ECC beam-column connection has shown flexural failure, ECC-SCC beam-column connection has shown combined shear and flexural failure at the connection towards the beam but their SCC counterparts beam exhibited non-ductile shear failure. Both ECC and ECC-SCC joints have shown high energy absorption capacity and ductility (more than 2000% and 1600%, respectively) as well as higher ultimate load and moment capacity with lower stiffness compared to their SCC counterparts. ECC and ECC-SCC beam-column connections have exhibited multi-cracking characteristics with lower crack width compared to those with SCC.

1. Introduction

In recent years numerous experimental studies have been performed on reinforced concrete (RC) beam-column connections to study the unexpected collapse and the behaviour of the joints. As a result, beam-column connections are critical components of the reinforced concrete structures (Parker and Bullman, 1997; Scott, 1992). While significant amount of research has been done on improving beam-column connection, large amount of these research are concentrated on new design concepts such as the anchorage system, reinforcements development length and geometry of beam-column connection. Experiments are conducted on exterior joints to explore the main reasons of non-ductile failure of beam-column connection and to evaluate their seismic performance (Ricci *et al.*, 2016, Alavi-Dehkordi et al., 2019, Lee et al., 2009, Barbhuiya and Choudhury, 2015). These researches showed that the shear strength of reinforced concrete beam-connection is influenced by the concrete strength, joint geometry, reinforcement confinement, column axial load and reinforcement bond condition (Hitoshi 2012, Park and Hadi 2012, Tran et al. 2014, Lima et al. 2012,Tran, 2016). There is a lack of study and research on applying new materials such as engineered cementitious composite (ECC) in RC building frames and beam-column connections (Pantelides et al. 2002, Qudah and Maalej 2014, Mangalathu and Jeon, 2018).

Lateral instability and collapse have been observed in non-ductile RC beam-column connections with inadequate design detail. Failure mode of beam-column connection can occur under different circumstances such as beam flexural failure, beam shear failure, column flexure failure and column shear failure (Allam et al. 2018). Therefore there should be adequate design procedures to have sufficient strength and deflection to maintain the structural integrity of the building system. Beam-column connection may experience large deformation and therefore, reduction of their vertical and horizontal load capacity can lead to partially or total collapse of structure (Pantelides et al. 2002, Walker 2001).

This paper presents the results of an experimental investigation on the structural performance of reinforced exterior beam-column connection incorporating ECC as conventional normal concrete replacement subjected to monotonic bending loading. The performance of ECC based beam-column connections compared to their SCC counterparts is described based on strength, moment-rotation/load-deformation response, energy absorbing capacity, ductility, stress-strain characteristics, cracking and failure modes.

2. Experimental test program

2.1. Description of test specimens

Three exterior reinforced beam-column connections made off with two different materials (SCC and ECC) designed according to CSA A23.3-14 standard were constructed and tested to study the effect of different materials on the performance of beam-column connections based on strength and ductility. Figure 1a and 1b shows design and detailing for the specimens.

For this study one joint specimen was constructed with full SCC material as control, and other exterior joints were made with full ECC and ECC-SCC (ECC material only used to depth of 160 mm in beam and column and other parts of members constructed using SCC). The details of sections are shown in Figure 1b.

All beams and columns had same cross section area of 120mm by 160mm width and height, respectively. Four 10M steel bars, two at the top and two at the bottom, were used as longitudinal reinforcement of beams and four 15M steel bars were used as longitudinal reinforcement of columns. 6M round steel bars were used as shear reinforcement for columns and in the beam-column connections. Beams had no shear reinforcement only one stirrup provided at the end of the beam to hold the longitudinal reinforcements. Detail of reinforcement and spacing are shown in Figure 1a.

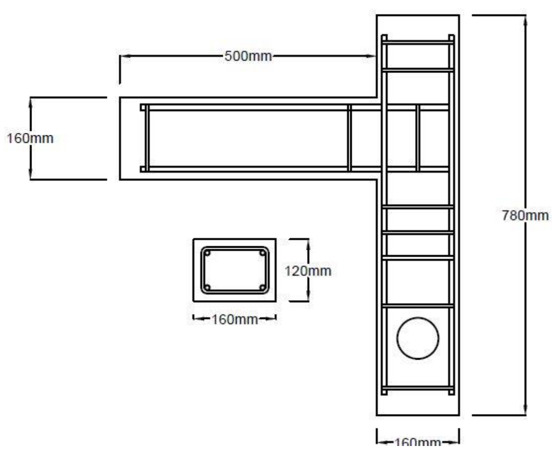

a) Reinforcement details

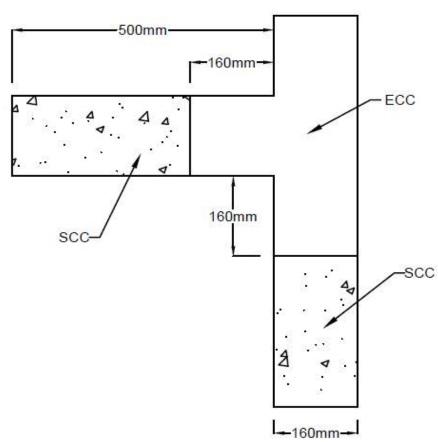

b) section details

Figure 1. Geometry and reinforcement details of exterior beam-column connection

2.2. Material properties

The ECC mix consisted of general purpose cement and fly ash (FA) as the cementing material, water, natural grain silica sand with 110 micrometer nominal size, Polyvinyl Alcohol (PVA) fibers and a polycarboxylate-based high range water reducer (HRWR) as shown in Table 1. The water to cementitious material ratio for ECC mix was 0.3 with PVA fiber content of 1% fibers/kg of dry material.

The PVA fibers are 39 microns in diameter and 8 mm in length with a tensile strength of 1620 MPa, modulus of elasticity of 42.8 GPa, and melting point of 225°C. PVA fiber geometry, dimension and specification are provided in Table 2 . For casting ECC, weighted solid contents except for the PVA fibers were introduced into the shear mixture and mixed for 1 minute. After compilation of dry mix, 75% of the water was added in combination with 50% of HRWR and mixed for additional 5 minutes. Then the remaining water and HRWR was introduced again with the same procedure to the mix, and mixed for another 5 minutes for the development of a uniform and consistent mixture. Lastly, the PVA fibers were added to the mortar for another 3 minutes of stirring until all fibers were dispersed with mixture.

A commercial SCC mixture made of 10 mm maximum size coarse aggregates, crushed sand, Portland cement and admixtures was used to cast joint specimens.

Table 1: Mix design of ECC

Mixture	Ingredients per 1 part of Cement					w/b
	Cement	Fly Ash (FA)	Silica Sand	PVA kg/m^3	HRWR kg/m^3	
ECC	1	1.2	0.80	26	5.4	0.27

*w: water; c: cement; b: binder

Table 2: Geometrical and mechanical properties of PVA

Fiber type	Length (mm)	Specific Gravity ($\frac{Kg}{m^3}$)	Melting point (℃)	Diameter (Microns)
PVA	8	1.3	225	38

To measure the average concrete compressive strength (f_c') three cylindrical specimens with dimensions of 100mm x 200mm at 28-days, as per ASTM C39 (2003) were tested and obtained results were summarized in Table 3. The four-point bending test was performed on the concrete prism specimens at 28-days according to ASTM c78 (2010). Typical load/flexural stress mid span deflection responses of ECC and SCC and flexural strength are presented in Figure 2 and Table 3, respectively. The properties of reinforcing steels were obtained based on tension test performed on three randomly selected specimens for each bar size and the results provided in Figure 3a, 3b and Table 4.

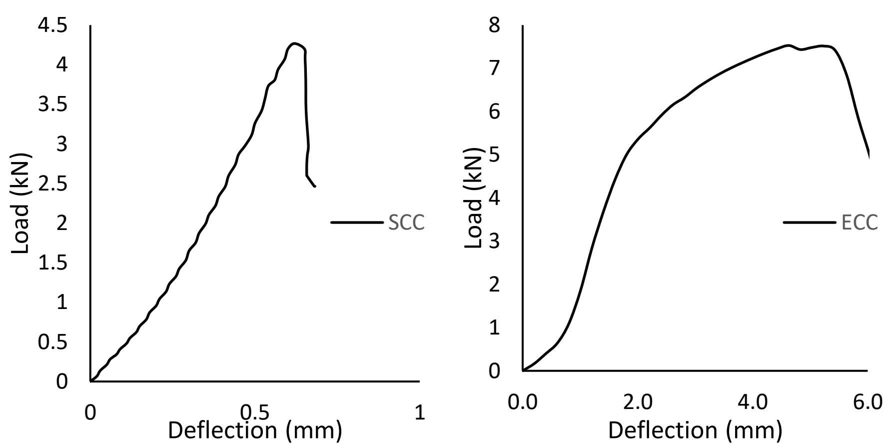

a) SCC b) ECC

Figure 2: Load-Deflection response of flexural specimens

Table 3: Concrete compressive and flexural strength

	SCC	ECC
Concrete compressive strength (MPa) at 28 days	80	69.5
Flexural strength (MPa) at 28 days	6.5	11.4

Table 4: Steel reinforcement yield stress and yield strain

Rebar size	Steel Yield stress (MPa)	Steel Yield strain (mm/mm)
15 M	475	2430
10 M	535	2290
6 M	597	2231

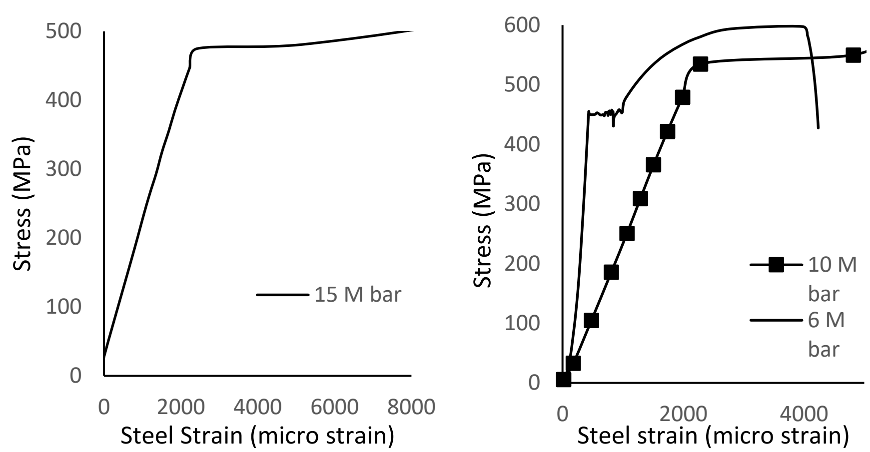

a) 15 M bar

b) 10 M bar and 6M bar

Figure 3: Stress-strain development of steel reinforcements

2.3. Instrumentation and test setup

All specimens were tested under monotonic load, applied at the free end of the beam as shown in Figure 4. Specimens were fixed to the foundation and connected to the strong floor of the laboratory. In order to measure the concrete and steel strain, strain gauges were attached to the column tension and compression side and to the beam compression zone (details are provided in Figure 4). Steel strain gauges were connected to longitudinal reinforcements of beam and column. Three LVDTs were used to measure beam and column deflection as shown in Figure 4. One LVDT was used to measure the beam deflection and two LVDTs were used to measure the maximum deflection of column and deflection at the centerline of beam-column connection. Two tilt meters were used to measure the rotation of beam and column as shown in Figure 4.

Vertical load was applied using a hydraulic jack fixed to the steel frame, connected to the strong floor of laboratory at the beam free end and the joint specimens were fixed to the foundation and connected to the strong floor of the laboratory. Details of test setup are provided in Figure 4.

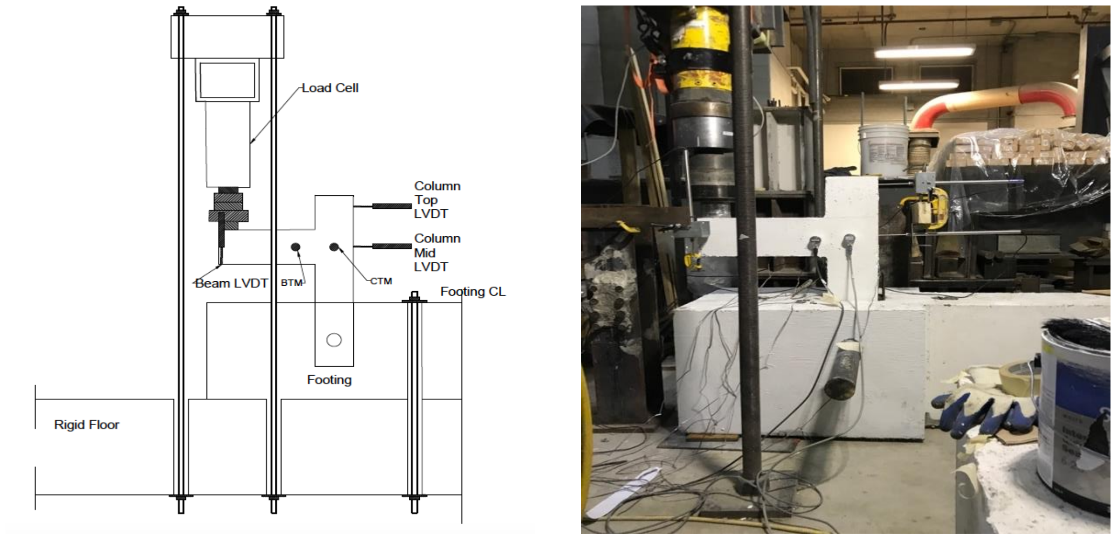

Figure 4: Test setup, locations of LVDTs and tilt meters

3. Result and discussion

3.1. Load-deflection and moment-rotation response

Figure 5 (a-b) present the load deflection behavior of experimentally tested exterior joints under bending. Specimen made from full section ECC had higher load capacity, higher beam deflection and beam rotation of 25.28 kN, 28.7 mm and 5.63 rad, respectively compared to specimens made from SCC and ECC-SCC. ECC-SCC specimen showed the lowest beam deflection, beam and column rotation 2.56 rad and 1.03 rad, respectively compared to ECC and SCC counterparts. Summary of ultimate load capacity, beam and column deflection and rotation for tested specimens is provided in Table 5.

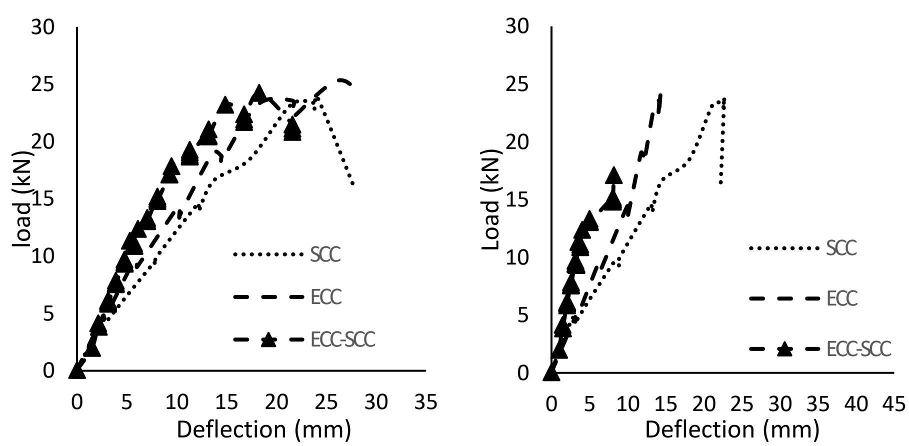

a) Beam vertical deflection b) Column horizontal deflection

Figure 5: Beam and column deflections

Beam and column rotation obtained from tilt meter are shown in Figure 6 (a-b). Maximum values of beam and column rotation for all specimens are summarized in Table 5.

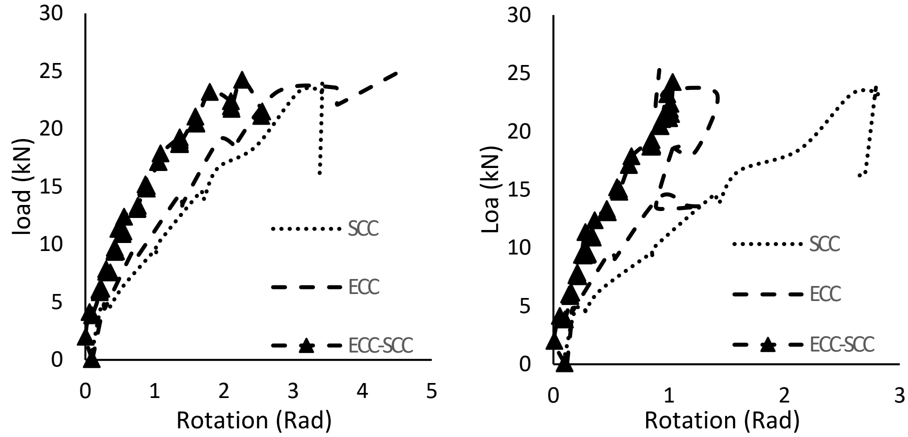

a) Beam rotation b) Column rotation

Figure 6: Beam and column rotation

Table 5: Summery of exterior joints ultimate load capacity, beam and column deflection and rotation

Specimen types	ultimate load (kN)	Beam deflection (mm)	Column deflection (mm)	beam rotation (rad)*	Column rotation (rad)*
SCC	23.87	27.77	22.69	3.42	2.80
ECC	25.28	28.70	14.45	5.63	1.42
ECC-SCC	24.24	21.61	10.12	2.56	1.03

*rotation obtained by tilt meter

Moment-rotation responses of beam and column (calculated) are shown in Figure 7 (a-b). ECC specimen had the highest moment-rotation for beam and column with higher moment capacity of 0.065 rad, 0.038 rad and 10.1 kN.m, respectively compared to ECC-SCC specimens with 0.045 rad, 0.0051 rad and 9.9 kN.m and SCC specimen with 0.043 rad, 0.046 rad and 7.38 kN.m.

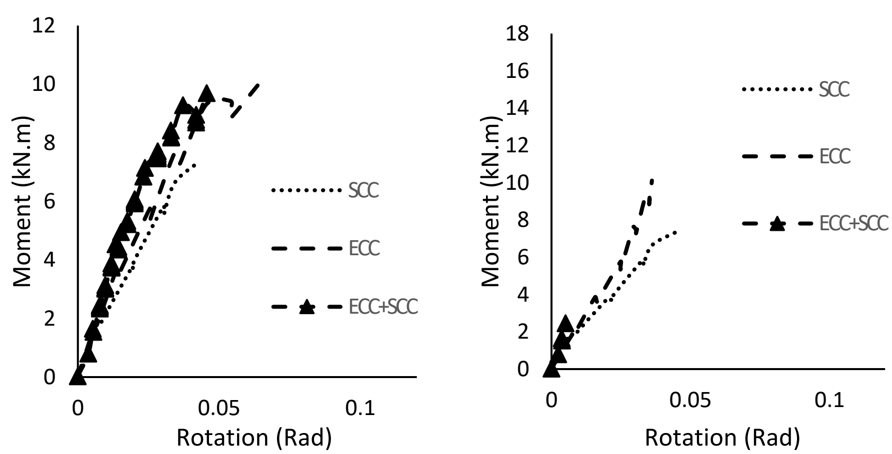

a) Beam moment-rotation b) Column moment-rotation

Figure 7: Beam and column moment-rotation

3.2. Ductility behavior, energy absorption capacity and stiffness of exterior joints

Table 6 provides summary of ductility, energy absorption capacity and stiffness for beam and column members of exterior joints. Stiffness calculated from the slope of flexural load-deflection curve. Energy absorption obtained from the area under flexural load-deflection curve up to the post peak load of 85% of the ultimate load. Ductility illustrated as the ratio of deflection at 85% of ultimate load after the peak load to 85% of the ultimate load before peak load. Beam-column connection made with ECC at the core of the joint showed higher ductility for both beam and column. Full ECC exterior showed relatively lower stiffness with 26% reduction compared to its counterparts. Energy absorption capacities of ECC and ECC-SCC specimens were increased by more than 2000% and 1600% with respect to their SCC control counterpart.

Table 6. Summary of ductility factor, energy absorption and stiffness of exterior beam-column connection

Specimen types	Ductility index beam	Ductility index column	Beam energy absorption capacity (J)	Column energy absorption capacity (J)	Beam stiffness (kN/mm)	Column stiffness (kN/mm)
SCC	1.1	1	12.92	22.9	1.43	1.38
ECC	1.8	1.2	297.6	42.4	1.06	1.37
ECC-SCC	1.8	1.1	219.1	26.8	1.32	2.88

3.3. Strain development in concrete and steel reinforcement

Concrete tension and compression strain developments for columns measured during test are reported in Figure 8a, and 8b. ECC sections in both ECC and ECC-SCC specimens reached highest tension and compression strain of 1200 micro strain and 1000 micro-strain, respectively while beams had higher concrete strain and failure of section occurred in the beam section. Beam's concrete tension strain reached to 1500 micro-strain for ECC and ECC-SCC specimens as shown in Figure 9 versus 614 micro strain in SCC control specimen. Details of ultimate strain for columns and beams for all specimens are provided in Table 7.

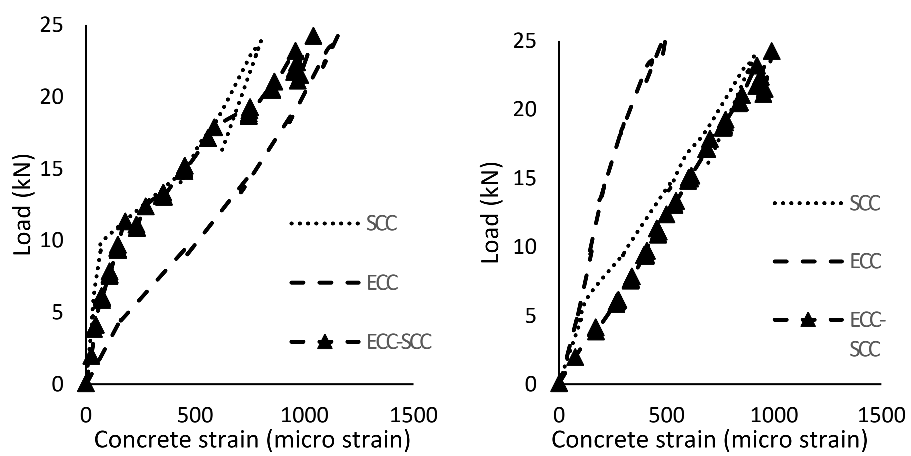

a) Column concrete tension strain b) Column Concrete compression strain

Figure 8: Columns concrete strain developments

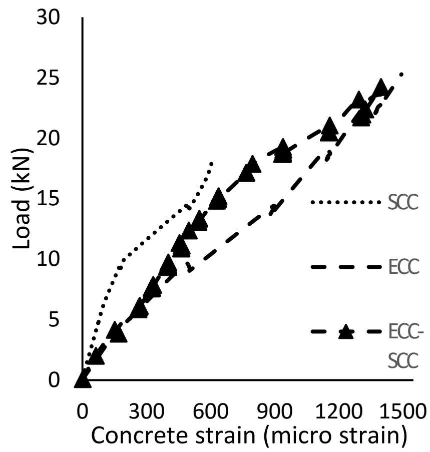

Figure 9: Beams concrete strain developments

Table 7: Beam and column concrete strain developments

Specimen types	Column		Beam
	Concrete tension strain (micro stain)	Concrete compression strain (micro strain)	Concrete tension strain (micro strain)
SCC	779	921	614
ECC	1186	485	1494
ECC-SCC	1042	989	1418

Strain developments in steel reinforcement measured for both beam and column are shown in Figure 10a and 10b. As SCC exterior joints failed under shear failure of beam member, longitudinal reinforcement didn't reach their yielding capacity. For ECC-SCC exterior joints, longitudinal reinforcement in the beam yielded and reached to the strain of more than 2500 micro strain as described before the ECC-SCC exterior joint failed under combined shear and flexure. Therefore the yielding of beam longitudinal reinforcement also confirmed the failure mode. Strain gauge of ECC specimen due to multiple cracking behaviour of ECC didn't gather correct strain development.

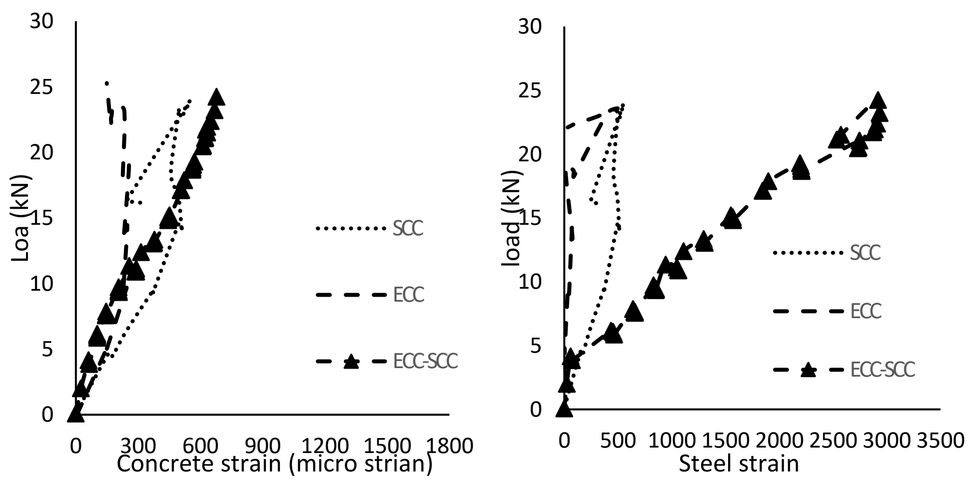

a) Column's steel strain developments b) Beam's steel strain developments

Figure 10: Beams and columns steel strain developments

3.4. Failure modes, crack patterns and crack widths

ECC exterior joint exhibited ductile flexural failure with cracks started from tension side of the beam and propagated towards the compression zone shown Figure 11. ECC-SCC specimen failed under combined shear and flexural failure. Flexural failure of ECC section of the ECC-SCC specimen started with cracks formation from the tension zone of the beam and propagated towards the compression face of the supporting column as shown in Figure 11. Shear failure of SCC section of the ECC-SCC specimen started with formation of shear cracks under the loading surface at free end of the beam and propagated towards ECC section of beam and ends at the contact surface of ECC-SCC which indicates higher shear capacity of ECC region. SCC exterior joint exhibited non-ductile joint shear failure prior to beam longitudinal reinforcement yielding. Crack pattern and failure modes shown in Figure 11.

a) ECC b) ECC-SCC c) SCC

Figure 11: Failure mode, crack pattern and crack widths

In ECC exterior joints, cracks mostly formed in the beam-column connection zone with the lowest crack width and highest crack number of 0.05 mm and 30 cracks respectively, while SCC specimen had lowest number of cracks (8 cracks) with largest average crack widths of 2 mm. Summary of failure modes, crack patterns and crack widths is provided in Table 8.

Table 8: Failure mode, crack pattern and crack width

Specimen types	Failure mode	Number of cracks	Maximum crack width	Average crack width (mm)
SCC	shear	8	3.5	2
ECC	flexure	30	1.5	0.05
ECC-SCC	combined shear-flexure	14	3	0.8

4. Conclusion

The following conclusions were drawn from the study:

- ECC and ECC-SCC exterior beam-column connection had higher ultimate load and moment rotation capacity. Exterior joint specimens made with full ECC section and ECC at the core of the joint had higher ductility with lower stiffness.
- Energy absorption capacities of ECC and ECC-SCC exterior beam-column connection were increased by more than 2000% and 1600%, respectively compared to their SCC exterior joint counterpart.
- ECC exterior connection showed ductile flexural joint failure under bending load, and ECC-SCC specimens failed under combined shear failure of SCC section and flexural failure of ECC core while SCC exterior joint exhibited non-ductile joint shear failure prior to beam longitudinal reinforcement yielding.

- Exterior beam-column connection made of ECC had highest number of cracks with lowest crack widths compared to its ECC-SCC and SCC counterparts.
- Concrete compression and tension strains of column for both ECC and ECC-SCC beam-column connection were higher than SCC beam-column connection. Beam concrete tension strains in both ECC and ECC-SCC beam-column connection were three times more than their SCC counterparts.
- Beam longitudinal reinforcements were yielded for both ECC and ECC-SCC while beam longitudinal reinforcements of SCC beam-column connection did not yield as the shear capacity of beam reached before its flexural capacity.

5. Acknowledgement

Authors acknowledge the financial support provided by the Natural Sciences and Engineering Research Council (NSERC) of Canada for this research.

6. References

ASTM C39, (2003). Standard test method for static modulus of elasticity and Poisson's ratio of concrete in compression. *American Society for Testing and Materials*, West Conshohocken, Pennsylvania, USA, 1-5.

ASTM C78 / C78M, (2010). Standard Test Method for Flexural Strength of Concrete (Using Simple Beam with Third-Point Loading), *American Society for Testing and Materials*, West Conshohocken, Pennsylvania, USA. pp. 1-4.

Alaee, P. and Li, B. (2017). High-strength concrete exterior beam-column joints with high-yield strength steel reinforcements, *Engineering Structures*. Elsevier Ltd, 145(May), pp. 305–321.

Alavi-Dehkordi, S., Mostofinejad, D. and Alaee, P. (2019) 'Effects of high-strength reinforcing bars and concrete on seismic behavior of RC beam-column joints', *Engineering Structures*. Elsevier, 183(July 2018), pp. 702–719.

Allam, S. M., Elbakry, H. M. F. and Arab, I. S. E. (2018) Exterior reinforced concrete beam column joint subjected to monotonic loading, *Alexandria Engineering Journal*. Faculty of Engineering, Alexandria University, 57(4), pp. 4133–4144.

CSA Standard A23.3-04. (2010). *Concrete Design Handbook*, 10th edition, Ontario, Canada: CSA.

Earthquake Engineering Research Institute (EERI), (1994). In: Hall JF, editor. Northridge earthquake January 17, preliminary reconnaissance report. Oakland, CA.

Hitoshi, S. (2012). Reinforced Concrete Beam-Column Joints: An Overlooked Failure Mechanism, ACI Struct. J. 109 pp. 65-74.

Lee, J. Y., Kim, J. Y. and Oh, G. J. (2009) Strength deterioration of reinforced concrete beam-column joints subjected to cyclic loading, *Engineering Structures*. Elsevier Ltd, 31(9), pp. 2070–2085.

Lima, C., Martinelli, E. and Faella, C. (2012). Capacity models for shear strength of exterior joints in RC frames: experimental assessment and recalibration, Bul'l. Earthq. Eng. 10(January), pp. 985-1007.

Mangalathu, S. and Jeon, J. S. (2018) Classification of failure mode and prediction of shear strength for reinforced concrete beam-column joints using machine learning techniques, *Engineering Structures*. Elsevier, 160(January), pp. 85–94.

Moehle, J.P., and Mahin S.A. (1991). Observations on the behavior of reinforced concrete buildings during earthquakes. ACI Special Publication 12767–90.

Pantelides C.P., Hansen, J., Nadauld, J., and Reaveley. L.D. Assessment of reinforced concrete building exterior joints with substandard details. PEER report 2002/ 18 Pacific Earthquake Engineering Research

Center College of Engineering University of California, Berkeley; May 2002

Parker, D.E. and Bullman, P.J.M. (1997). Shear strength within reinforced concrete beam-column joints, Struct. Eng. 75 (4) 53–57.

Park, S. and Mosalam, K. M. (2012). 'Analytical Model for Predicting Shear Strength of Unreinforced Exterior Beam-Column Joints', ACI Struct. J. 109 pp.149-159.

Qudah, S. and Maalej, M. (2014) Application of Engineered Cementitious Composites (ECC) in interior beam-column connections for enhanced seismic resistance, *Engineering Structures*. Elsevier Ltd, 69(April), pp. 235–245.

Ricci, P. *et al.* (2016) Experimental tests of unreinforced exterior beam-column joints with plain bars, *Engineering Structures*. Elsevier Ltd, 118(March), pp. 178–194.

Scott, R.H. 1992. The effects of detailing on reinforced concrete beam- column connection behaviour, Struct. Eng. 70 (18) 318– 324.

Barbhuiya, S. and Choudhury, A. M. (2015) A study on the size effect of RC beam-column connections under cyclic loading, *Engineering Structures*. Elsevier Ltd, 95(March), pp. 1–7.